H. Abdalla ... R. Blackwell ... P. deWilt ... J. Hawkes ... J. Lau ... G. Rowell ... F. Voisin ... et al. (H.E.S.S. Collaboration)

H.E.S.S. limits on linelike dark matter signatures in the 100 GeV to 2 TeV energy range close to the Galactic Center

Physical Review Letters, 2016; 117(15):151302-1-151302-7

for the construction of the background PDF, a major component in the likelihood discussed below.

The likelihood function is composed of a Poisson normalization term (based on the total number of events in the signal and background regions) and a spectral term related to the expected spectral contribution of the signal and the background component in the analysis region of interest (ROI). A description of this approach, called the full likelihood method below, is given in Ref. [19].

The likelihood formula reads

$$\mathsf{L}(N_{\rm signal}, N_{\rm bckg} | N_{\rm ON}, N_{\rm OFF}, E_i) = \frac{(N_{\rm signal}+N_{\rm bckg})^{N_{\rm ON}}}{N_{\rm ON}!} e^{-(N_{\rm signal}+N_{\rm bckg})} \times \frac{(\alpha N_{\rm bckg})^{N_{\rm OFF}}}{N_{\rm OFF}!} e^{-\alpha N_{\rm bckg}} \times \prod_{i=1}^{N_{\rm ON}} (\eta \times {\rm PDF}_{\rm signal}(E_i) + (1-\eta) \times {\rm PDF}_{\rm bckg}(E_i)), \quad (1)$$

where $N_{\rm ON}$ and $N_{\rm OFF}$ are the measured number of events in the signal and background regions, α is the exposure ratio between the background and signal regions, E_i (with $i \in [1, N_{\rm ON}]$) represents a vector of energies of events measured in the signal region, and $\eta = N_{\rm signal}/(N_{\rm signal} + N_{\rm bckg})$ is the line signal fraction in the ON region sample. $\rm PDF_{signal}$ and $\rm PDF_{bckg}$ are the probability density functions for the signal and background components that refer to measured energy spectra, that is, photon energies smeared by the instrument response functions (IRFs). $\rm PDF_{signal}$ is obtained from dedicated monoenergetic gamma-ray simulations of signals for each DM particle mass considered in the analysis. $\rm PDF_{bckg}$ corresponds to the best fit of the normalized energy distribution of events reconstructed in the OFF regions. No additional term corresponding to the fit of $\rm PDF_{bckg}$ was added to the likelihood formula (1). The number of signal ($N_{\rm signal}$) and background ($N_{\rm bckg}$) events are free parameters of the model, while additional information on the signal and background spectral shape is included in the fit. The line energy position $E_{\rm line}$ is kept fixed, and the line signal fraction η that represents the relative contribution of the signal in the analyzed region is fitted.

The IRFs were obtained from the full gamma-ray MC simulations of the gamma-ray showers and of the H.E.S.S. instrument. They were employed in the dedicated MC simulations to derive the expected measured energy distributions leading to $\rm PDF_{signal}$ and $\rm PDF_{bckg}$. An optimal circular signal region of 0.4° radius was found using the method of Rolke *et al.*, [20], corresponding to a solid angle of $\Delta\Omega = 1.531 \times 10^{-4}$ sr.

The resulting sensitivity estimates computed with MC simulations for a line scan between 100 GeV and 2 TeV as well as the 95% confidence level (C.L.) limits derived from the data sample are presented below.

Results.—At first, a search for an excess in the ON-source region was performed by using OFF-region empty field data. It should be noted that despite the signal region being displaced from the Galactic Center (GC) position, the 130 GeV excess ROI may still be subject to contributions from surrounding astrophysical sources. In particular, the bright extended source HESS J1745-303 [21] was excluded (a mask of 0.4°) while the contribution from HESS J1741-302 [22] was estimated to be negligible. The significance map shown in Fig. 1 was reconstructed with an annular background region [11] around the signal region for the 15.2 h data set. In the absence of any genuine gamma-ray signal in the field of view, the significances derived from background fluctuations follow a Gaussian distribution with a width of 1, as is the case once the significant excess at the position of HESS J1745-290 [23] is excluded, coincident with the supermassive black hole SgrA*. As also shown in Fig. 1, no significant excess ($N_{\rm signal}$) was found in the 0.4° radius ROI at the best-fit position of the 130 GeV excess $(l, b) = (-1.5°, 0°)$.

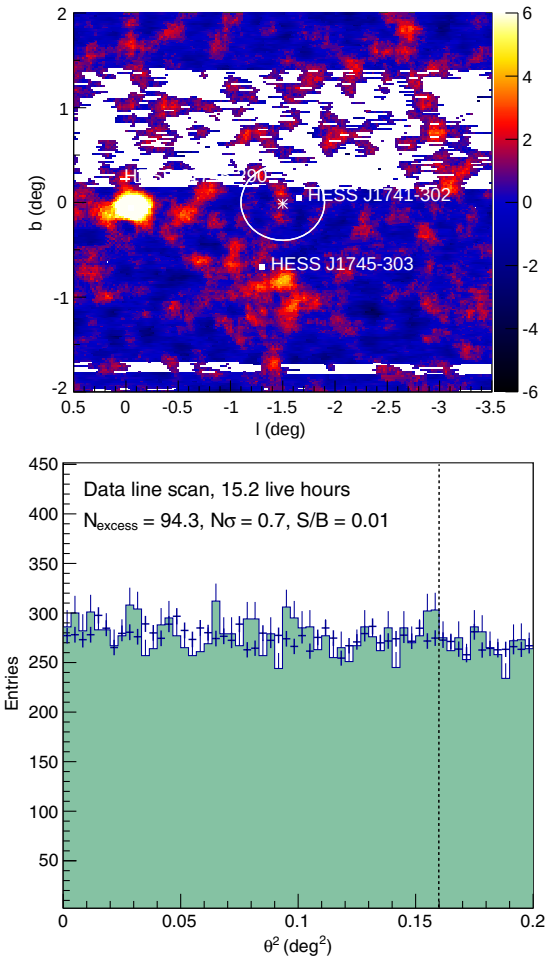

FIG. 1. Significance map presented in Galactic coordinates (top) and emission angle square θ^2 distribution (bottom) in the considered ROI. The ROI is expressed in the map with a white circle centered on the 130 GeV excess (−1.5°, 0°) marked with a white cross. The known source HESS J1745-290 is detected, even at a large angular offset. The dashed vertical line in the bottom shows the θ cut of 0.4°.

Therefore, upper limits were derived for a linelike signal in the energy range from 100 GeV to 2 TeV.

The number of measured background events in the ROI of 0.4° and the $\mathrm{PDF}_{\mathrm{bckg}}$ parametrization were derived from the measured energy distributions in the data control OFF-source regions symmetrically surrounding the 130 GeV excess. The likelihood fits covered two predefined energy ranges from 80 GeV to 1 TeV and from 200 GeV to 3 TeV, which allowed our observations to probe line signals with energy from 100 to 500 GeV and from 500 GeV to 2 TeV, respectively, ensuring a large energy lever arm in the fit in each case. For each line energy, upper limits on η and subsequently on the number of excess events N were obtained using Eq. (1). The $\eta^{95\%\,\mathrm{C.L.}}$ upper-limit value was obtained from a one-sided cut on the log-likelihood function corresponding to its increase by 2.71. To derive the sensitivity expectations, we use the median of the 95% C.L. upper limit distributions obtained from a large number of simulations performed assuming 15.2 and 112 h of time exposure.

The limits on the flux Φ and on the DM velocity averaged annihilation cross section $\langle\sigma v\rangle$ were derived as

$$\Phi^{95\%\,\mathrm{C.L.}} = \frac{N_\gamma^{95\%\,\mathrm{C.L.}}}{T_{\mathrm{OBS}}} \times \frac{\int_{E_{\mathrm{min}}}^{E_{\mathrm{max}}} dN/dE_\gamma(E_\gamma)dE_\gamma}{\int_{E_{\mathrm{min}}}^{E_{\mathrm{max}}} A_{\mathrm{eff}}(E_\gamma)dN/dE_\gamma(E_\gamma)dE_\gamma}, \tag{2}$$

$$\langle\sigma v\rangle^{95\%\,\mathrm{C.L.}} = (8\pi m_{\mathrm{DM}}^2/2\Phi_{\mathrm{astro}}) \times \Phi^{95\%\,\mathrm{C.L.}}, \tag{3}$$

where T_{OBS} is the observation time, A_{eff} and dN/dE are, respectively, the effective area for gamma rays and the differential energy spectrum of the expected DM signal expressed as functions of the true energy, m_{DM} is the DM particle mass, and $[E_{\mathrm{min}}, E_{\mathrm{max}}]$ are the bounds of the energy range. The astrophysical factor Φ_{astro} is given by the integral of the squared DM density along the line of sight and solid angle Ω. A dark matter distribution following an Einasto profile [24] with halo parameters given in Ref. [3] has been considered at the center of the ROI resulting in the value of $\Phi_{\mathrm{astro}} = 2.46 \times 10^{21}\ \mathrm{GeV^2\,cm^{-5}}$. For DM annihilating into two gamma rays, the differential energy spectrum is $dN/dE_\gamma \sim 2\delta(E_\gamma - m_\chi)$, where the factor of 2 results from the annihilation of DM particles into two photons.

Limits on the flux per steradian and on $\langle\sigma v\rangle$ obtained from MC simulations and those calculated with the 15.2 h of data are presented in Figs. 2 and 3, respectively, and show the potential of the applied method for the DM line signal detection. The measured limits are in good agreement with the expected sensitivity. The limits obtained with H.E.S.S. II for a DM density profile centered on the 130 GeV excess position efficiently complement previous limits of H.E.S.S. I [3] and cover the gap in mass between 300 and 500 GeV, even though the H.E.S.S. II results are derived for a different location in the sky. Because of differences in the analysis methods and a limited size of the current data sample a combination of the results obtained by H.E.S.S. phase I and phase II was not performed.

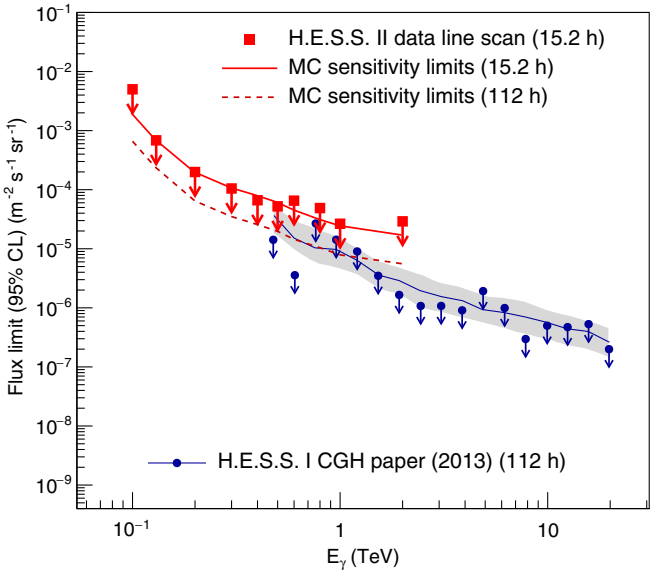

FIG. 2. Flux limits at 95% C.L. for a line scan between 100 GeV and 2 TeV. The results obtained from 15.2 h of data are represented by points in red. The red dashed line represents the limits expected for 112 h of observation time, calculated as the median limits from 500 simulated data sets. The red solid line is given for 15.2 h MC simulations. Former limits from H.E.S.S. I [3] obtained in the Central Galactic Halo (CGH) region are represented as blue data points (the gray band displaying the level of systematic uncertainties).

The case of the DM halo centered on the GC was also analyzed and the results are shown in Fig. 3, keeping the ROI on the 130 GeV excess position. The decrease in sensitivity by a factor of 8 to 10 can be explained by a decrease in the Φ_{astro} value by a factor of 4.3 ($\Phi_{\mathrm{astro}} = 5.6 \times 10^{20}\,\mathrm{GeV^2\,cm^{-5}}$). In this case the DM signal leakage into the OFF regions was 40%, adding another factor of 2 in the total loss in sensitivity for the line search studies with a data sample dedicated to the 130 GeV excess.

For the particular case of the 130 GeV excess, the likelihood method yielded the 95% C.L. limit on the line signal fraction η of 0.0083 leading to an $N_\gamma^{95\%\,\mathrm{C.L.}}$ of 102.8 events. The 95% C.L. upper limits on the flux and $\langle\sigma v\rangle$ for data and MC simulations are summarized in Table I for both Einasto [24] and Navarro-Frenk-White (NFW) [26] DM halo profiles.

The cross-check studies with independent calibration and reconstruction, here in monoscopic mode, confirmed the conclusion of no significant excess at 130 GeV and the exclusion at 95% C.L. for the 130 GeV excess. Because of the large extension of the galactic DM halo, a fraction of the expected DM signal leaks into the background regions, found to be at the level of 25% of the DM signal in the ROI. The presented $\langle\sigma v\rangle$ limits account for this effect. The

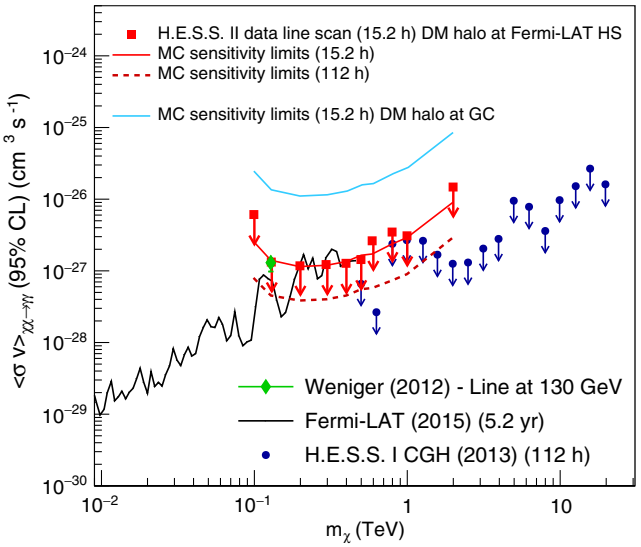

FIG. 3. $\langle\sigma v\rangle$ limits at 95% C.L. (red points) for the line scan between 100 GeV and 2 TeV, derived from 15.2 h of data and using an Einasto DM profile with a Φ value calculated with the CLUMPY package [25] ($\rho_s = 20$ kpc, $r_s = 0.17$). The MC estimations are presented with the same conventions as in Fig. 2. The former limits from H.E.S.S. I [3] obtained in the CGH region and the *Fermi* LAT [10] are represented by blue and black data points, respectively. The $\langle\sigma v\rangle$ value corresponding to the 130 GeV line feature reported as R16 in Ref. [7] is shown in green. The limits extracted with the assumption of the DM halo position at the GC are shown with a continuous blue line (see the text). It should be noted that the comparison of the limits on the hot spot obtained in this work cannot be directly done with the H.E.S.S. I results as the DM halo was centered on the Galactic Center position in the sky. In case of the *Fermi* LAT, the red curve can still be compared to the *Fermi* LAT limits as the latter would only be marginally modified (at the level of 1%) by the displacement of the DM halo, given the very large size of the ROI (16° of radius) in use.

impact of various systematic uncertainties was evaluated with full MC simulations including those of radial acceptance effects within the signal region and were found to only affect the limits obtained at the few percent level. As the signal region is sufficiently large there is no effect due to the point spread function. Finally, to estimate the impact of systematic uncertainties in the limits calculation for the considered sources of errors such as IRF values, the global energy scale, the background PDF shape, and the diffuse emission component included in the background regions, nuisance parameters modeled with Gaussian functions were introduced in the full likelihood calculations. The impact of each systematic effect was studied with 500 MC simulations providing statistically calibrated results. The background PDF shape has been identified as the dominant source of systematic uncertainties, changing 95% C.L. limits by 10% to 15% depending on the line energy probed.

TABLE I. 95% C.L. limits on the flux (per solid angle unit) and $\langle\sigma v\rangle$ for the detection of the 130 GeV line. The limits on $\langle\sigma v\rangle$ are given for Einasto and NFW DM halo profiles. The MC values are coming from the simulations of 15.2 h of observation time. The quoted values do not include the systematic effects.

	$\Phi^{95\%\,\mathrm{C.L.}}/\Delta\Omega$ $10^{-4}\gamma\ \mathrm{m}^{-2}\ \mathrm{s}^{-1}\ \mathrm{sr}^{-1}$	$\langle\sigma v\rangle^{95\%\,\mathrm{C.L.}}$. $10^{-27}\ \mathrm{cm}^3\ \mathrm{s}^{-1}$ Einasto profile	$\langle\sigma v\rangle^{95\%\,\mathrm{C.L.}}$. $10^{-27}\ \mathrm{cm}^3\ \mathrm{s}^{-1}$ NFW profile
Data	8.4	1.38	1.43
MC	8.6	1.42	1.56

Summary and conclusions.—Analysis of data from dedicated H.E.S.S. II observations of 18 h towards the vicinity of the Galactic Center lead to the 95% C.L. exclusion of the $\langle\sigma v\rangle$ value associated with the 130 GeV excess reported in Ref. [7] in the *Fermi*-LAT data. The likelihood method developed for this study has been successfully applied to estimate for the first time the sensitivity for a DM line search with the five telescope configuration of the H.E.S.S. experiment. New constraints on linelike DM signals have been obtained in the line scan in the energy range between 100 GeV and 2 TeV, bridging the gap between previously reported H.E.S.S. phase I and *Fermi*-LAT results. The analysis reported here has been performed under the hypothesis of the DM halo centered at the 130 GeV excess position, displaced with respect to the gravitational center of the Galaxy. Moving the center of the DM halo to $l = 0$, $b = 0$ implies a loss of sensitivity by a factor of at least 8 for the line search studies. The conclusions about the sensitivity of H.E.S.S. in phase II remain valid for explorations close to the Galactic Center and the current method will be employed on larger observational data sets in the future.

The support of the Namibian authorities and of the University of Namibia in facilitating the construction and operation of H.E.S.S. is gratefully acknowledged, as is the support by the German Ministry for Education and Research (BMBF), the Max Planck Society, the German Research Foundation (DFG), the French Ministry for Research, the Centre National de la Recherche Scientifique-Institut National de Physique Nucléaire et de Physique des Particules and the Astroparticle Interdisciplinary Programme of the Centre National de la Recherche Scientifique, the United Kingdom Science and Technology Facilities Council (STFC), the Institute of Particle and Nuclear Physics of the Charles University, the Czech Science Foundation, the Polish Ministry of Science and Higher Education, the South African Department of Science and Technology and National Research Foundation, and the University of Namibia. We appreciate the excellent work of the technical support staff in Berlin, Durham, Hamburg, Heidelberg, Palaiseau, Paris, Saclay, and Namibia in the construction and operation of the equipment. R. C. G. Chaves Funded by European Union Seventh Framework Programme Marie Curie, Grant Agreement No. PIEF-GA-2012-332350.

*Deceased.
†Corresponding authors.
contact.hess@hess-experiment.eu

[1] G. Bertone, D. Hooper, and J. Silk, Phys. Rep. **405**, 279 (2005).
[2] J. Conrad, J. Cohen-Tanugi, and L. E. Strigari, J. Exp. Theor. Phys. **121**, 1104 (2015).
[3] A. Abramowski *et al.* (H.E.S.S. Collaboration), Phys. Rev. Lett. **110**, 041301 (2013).
[4] W. B. Atwood *et al.* (Fermi-LAT Collaboration), Astrophys. J. **697**, 1071 (2009).
[5] T. Bringmann, X. Huang, A. Ibarra, S. Vogl, and C. Weniger, J. Cosmol. Astropart. Phys. 07 (2012) 054.
[6] T. Bringmann and C. Weniger, Phys. Dark Univ. **1**, 194 (2012).
[7] C. Weniger, J. Cosmol. Astropart. Phys. 08 (2012) 007.
[8] M. Su and D. Finkbeiner, arXiv:1206.1616.
[9] M. Ackermann *et al.* (*Fermi*-LAT Collaboration), Phys. Rev. D **88**, 082002 (2013).
[10] M. Ackermann *et al.* (*Fermi*-LAT Collaboration), Phys. Rev. D **91**, 122002 (2015).
[11] F. Aharonian *et al.* (H.E.S.S. Collaboration), Astron. Astrophys. **457**, 899 (2006).
[12] J. Bolmont *et al.*, NIM A **761**, 46 (2014).
[13] M. Holler *et al.* (H.E.S.S. Collaboration), Proc. Sci., ICRC2015 (**2016**) 980.
[14] T. Murach *et al.* (H.E.S.S. Collaboration), Proc. Sci., ICRC2015 (**2016**) 1022.
[15] R. D. Parsons *et al.* (H.E.S.S. Collaboration), Proc. Sci., ICRC2015 (**2016**) 826.
[16] M. Holler *et al.* (H.E.S.S. Collaboration), Proc. Sci., ICRC2015 (**2016**) 847.
[17] R. D. Parsons *et al.* (H.E.S.S. Collaboration), Proc. Sci., ICRC2015 (**2016**) 830.
[18] M. de Naurois and L. Rolland, Astropart. Phys. **32** (2009) 231.
[19] J. Aleksic, J. Rico, and M. Martinez, J. Cosmol. Astropart. Phys. 10 (2012) 032.
[20] W. A. Rolke, A. M. López, and J. Conrad, Nucl. Instrum. Methods Phys. Res., Sect. A **551**, 493 (2005).
[21] F. Aharonian *et al.* (H.E.S.S. Collaboration), A&A **483**, 509 (2008).
[22] O. Tibolla, N. Komin, K. Kosack, M. Naumann-Godo, F. A. Aharonian, W. Hofmann, and F. Rieger, AIP Conf. Proc. **1085**, 249 (2008).
[23] F. Acero *et al.*, Mon. Not. R. Astron. Soc. **402**, 1877 (2010).
[24] V. Springel, J. Wang, M. Vogelsberger, A. Ludlow, A. Jenkins, A. Helmi, J. F. Navarro, C. S. Frenk, and S. D. M. White, Mon. Not. R. Astron. Soc. **391**, 1685 (2008).
[25] http://adsabs.harvard.edu/abs/2012CoPhC.183..656C; http://cdsads.u-strasbg.fr/abs/2015arXiv150607628B.
[26] J. F. Navarro, C. S. Frenk, and S. D. M. White, Astrophys. J. **490**, 493 (1997).